Pyroelectric Infrared Detectors

1. Principal set-up

Figure 1 shows the principle set-up of a pyroelectric infrared detector. Components are the responsive element and the preamplifier whose essential elements are integrated in the detector. The sensitive element consists of a pyroelectric chip which is thin and covered with electrodes. In some cases an absorption layer is applied to the front of the responsive element to improve its absorption behavior.

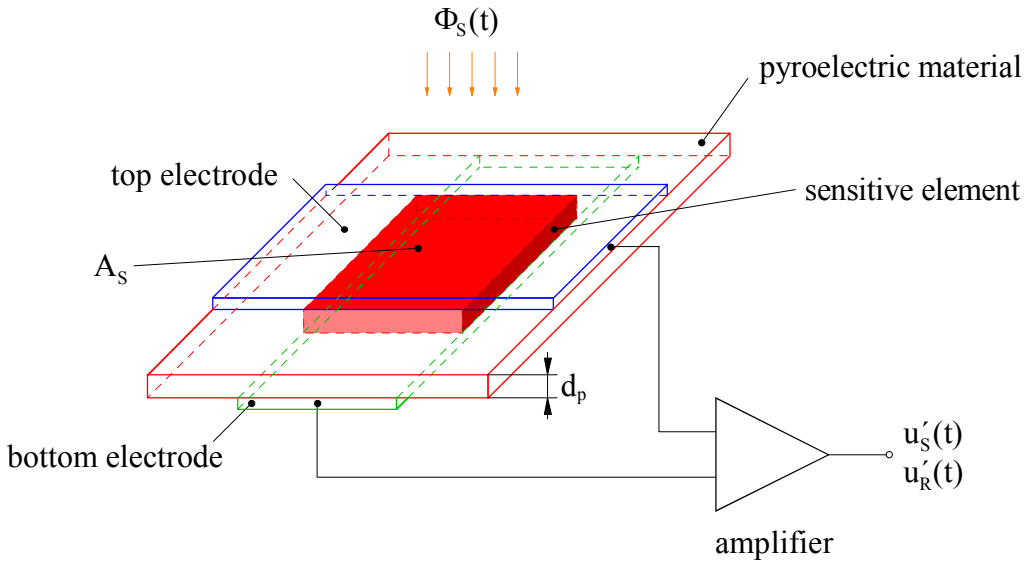

Figure 1: Principle set-up of a pyroelectric infrared detector

The incident radiation flux $\Phi_S(t)$ hits the radiation-sensitive element with the area A_S and absorption coefficient α. The absorption of radiation flux results in a temperature change $\Delta T(t)$ within the pyroelectric material. The pyroelectric effect generates charges $\Delta Q(t)$ on the electrodes. These charges are transformed into a signal voltage $u_S'(t)$.

Various noise sources in the pyroelectric chip and the preamplifier generate a noise voltage $u_R'(t)$ at the detector output. This voltage limits the radiation flux, which can be detected in the minimum.

2. Detector characteristics

The essential characteristics of pyroelectric detectors are the responsivity S_V, the noise equivalent power NEP and the specific detectivity D^*. They are defined in the steady-state condition for sinusoidal processes. They generally depend on modulation frequency f, wavelength λ and detector temperature T.

a) Responsivity

The responsivity S_V is defined as:

$$S_V = \frac{\widetilde{u}'_S}{\widetilde{\Phi}_S} \qquad \text{[V/W]} \qquad (1)$$

where: $\widetilde{\Phi}_S$ rms value of the sinusoidally modulated radiation flux

$\widetilde{u}'_S$ rms value of the sinusoidal signal voltage at the detector output.

b) Noise equivalent power

The noise equivalent power NEP characterises the signal-to-noise ratio of the detector:

$$NEP = \frac{\widetilde{u}'_R}{S_V} \qquad \text{[W]} \qquad (2)$$

where: $\widetilde{u}'_R$ rms value of the noise voltage at the detector output.

The combination of the equations (1) and (2) shows that the noise equivalent power represents the minimum detectable power of the detector, and is given by a ratio of 1 between signal voltage and noise voltage ($\widetilde{u}'_S / \widetilde{u}'_R = 1$).

c) Specific detectivity

The specific detectivity characterises also the signal-to-noise ratio:

$$D^* = \frac{\sqrt{A_S B}}{NEP} = \frac{\sqrt{A_S}\, S_V}{\widetilde{u}'_{Rn}} \qquad \text{[cmHz}^{1/2}\text{/W]} \qquad (3)$$

where: $\widetilde{u}'_{Rn} = \widetilde{u}'_R / \sqrt{B}$ $\qquad \text{[V/Hz}^{1/2}\text{]} \qquad (4)$

$\widetilde{u}'_{Rn}$ effective value of the noise voltage at the preamplifier output normalized on a bandwidth B = 1 Hz.

The definition of the specific detectivity allows a simple comparison between the D* value of the real sensor and the theoretical D* limit. This limit depends only on nature constants (Boltzmann constant k, Stefan-Boltzmann constant σ) and the temperature T:

$$D^*_{\max} = 1/\sqrt{16 k \sigma T^5} \qquad (5)$$

For a temperature of 300 K this value amounts to:

$$D^*_{\max} = 1{,}8 \cdot 10^{10} \text{ cmHz}^{1/2}\text{/W} \ .$$

3. Pyroelectric material

The pyroelectric material takes a fundamentally position as the real transducer element in the pyroelectric radiation detector. Of 32 existing crystal classes crystals with the point group balance 1, m, 2, mm2, 3, 3 m, 4, 4 mm, 6 and 6 mm have a so-called spontaneous polarization which makes the appearance of the pyroelectric effect possible. Crystals of these crystal classes are called pyroelectric materials. Pyroelctric materials at which the spontaneous polarization can appear only in one single direction in the crystal (uniaxial pyroelectric materials) are technically meaningful. The crystal classes 2, mm2, 3, 3 m, 4, 4 mm, 6 and 6 mm, are included. The direction of the spontaneous polarization and the polar axis of the crystal are the same.

For use in pyroelectric radiation detectors the following material characteristics of the pyroelectric material are of importance:

p	pyroelectric coefficient
ε_r	dielectric constant
tanδ	dielectric loss
c_P'	volume-specific heat capacity

For high values of responsivity S_V and specific detectivity D* a big pyroelectric coefficient p and small values of dielectric constant ε_r, dielectric loss tan δ and volume-specific heat capacity c_P' are required.

For many years the pyroelectric material lithium tantalate ($LiTaO_3$) has proved itself at use in pyroelectric detectors. It fulfils not only the demands on material characteristic quantities just mentioned but also stands out due to an excellent temperature stability and very good reproducibility of the detector performance.

Typical material properties of $LiTaO_3$ at room temperature are:

$p = 1{,}8 \cdot 10^{-8}\ Ccm^{-2}K^{-1}$
$\varepsilon_r = 43$
$tan\delta = 0{,}001$
$c_P' = 3{,}2\ Jcm^{-3}K^{-1}$

4. Equivalent electric circuits of the responsive element and preamplifier

The absorption of the radiant flux Φ_S causes a temperature change ΔT in the pyroelectric material. This temperature change ΔT generally depends on the place in the pyroelectric material. This local dependence can be often neglected in good approximation. The thermal behavior of the responsive element can be represented in these cases by a simple analogous electrical substitute circuit diagram (figure 2) with heat capacity

$$H_P = c_P' d_P A_S \qquad (6)$$

where: d_P thickness of the responsive element

and thermal conductance G between the sensitive element and his surroundings.

Because of the statistical behaviour of the heat exchange between responsive element and surrounding a so-called temperature noise is produced. Therefore in figure 2 an additional noise source is included, with:

$$\tilde{p}_{RnT} = \sqrt{4kT^2G} \tag{7}$$

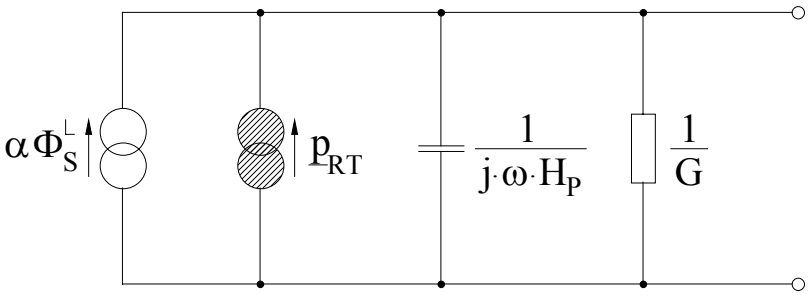

Figure 2: Analogous electric circuit of the responsive element at simplified thermal conditions

The temperature variation ΔT leads to a pyroelectric current which flows at short circuit of the electrodes of the sensitive element. This pyroelectric current arises under consideration of the definition of the pyroelectric coefficient and the thermal conditions according to figure 2:

$$\hat{i}_P^{\angle} = \frac{\alpha p \hat{\Phi}_S}{c'_P d_P} T_R \tag{8}$$

with

$$T_R = \frac{j\omega\tau_T}{1 + j\omega\tau_T} \tag{9}$$

$$\tau_T = H / G \tag{10}$$

$$\omega = 2\pi f \tag{11}$$

The dimensionless function T_R is called complex normalized current responsivity. For a sensitive element isolated ideally thermally (G = 0) the complex normalized current responsivity reaches the value 1. For most sensor constructions and for practically interesting modulation frequencies f = 1…1000 Hz this value 1 is a good approximation, if the thermal time constant τ_T has corresponding values. If the incident radiation is not modulated (f = 0), no pyroelectric current is produced. A pyroelectric detector is not responsible for a constant radiation. He always needs a temporal modulation of the incident radiant flux e.g. by chopping.

Figure 3 shows the electrical circuit of the responsive element. Input quantity is the pyroelectric current after equation (8). Substitute elements are the electrical capacity

$$C_P = \frac{\varepsilon_o \varepsilon_r A_S}{d_P} \quad , \tag{12}$$

the frequency dependent resistance

$$r_P = 1/(\omega C_P \tan\delta) \tag{13}$$

and the so-called tanδ noise source

$$\tilde{i}_{RnD} = \sqrt{4kT\omega C_P \tan\delta} \quad . \tag{14}$$

It describes thermal noise of the element resistance r_P.

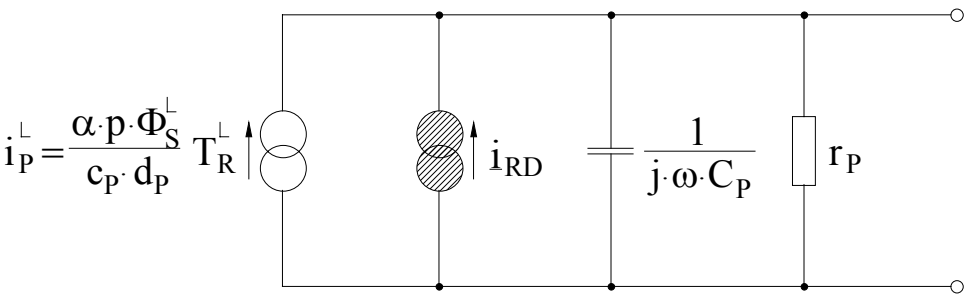

Figure 3: Electrical circuit of the responsive element

In figures 4 and 5 the electrical circuits of two fundamental preamplifier variants (preamplifier in voltage mode or current mode) are represented. Substitute elements are in both cases the input resistance r_{eV} and input capacitance C_{eV} as well as current noise and voltage noise $\tilde{i}_{RnV}$ or $\tilde{u}_{RnV}$ of the preamplifier. The thermal noise of the input resistance is desciped by noise source:

$$\tilde{i}_{RnR} = \sqrt{\frac{4kT}{r_{eV}}} \quad . \tag{15}$$

If the preamplifier is operated in voltage mode, gain v_V must be taken into account. The preamplifier in current mode contains a negative feedback op-amp (gain → ∞) with resistor R_{GK}, his capacity C_{GK} and his thermal noise:

$$\tilde{i}_{RnGK} = \sqrt{\frac{4kT}{R_{GK}}} \quad . \tag{16}$$

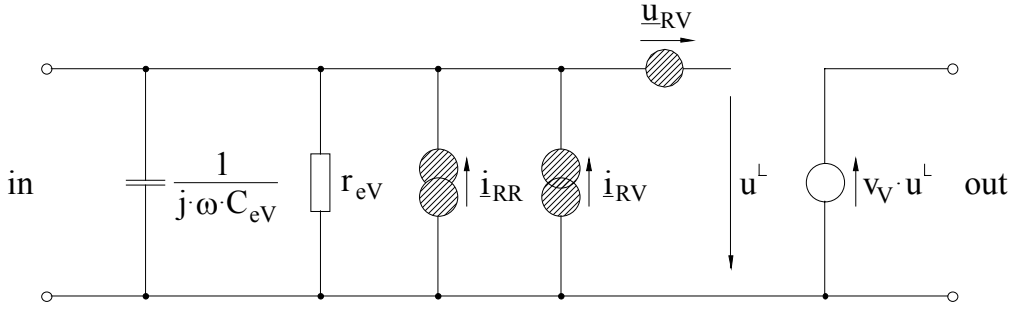

Figure 4: Electrical circuit of a preamplifier in voltage mode

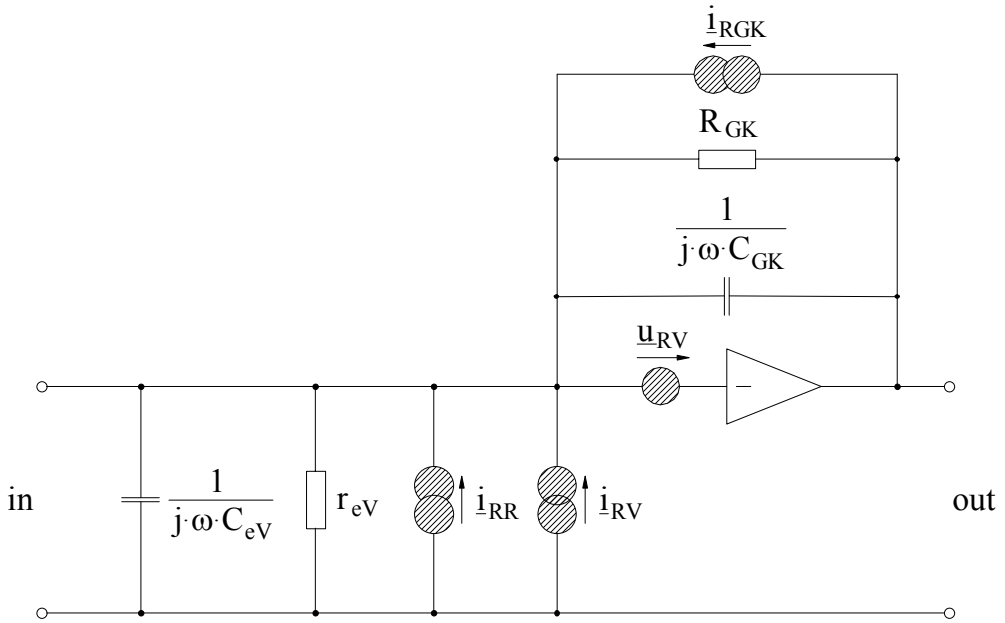

Figure 5: Electrical circuit of a preamplifier in current mode

5. Responsivity

According to the defining equation (1) the responsivity S_V in voltage mode is given by:

$$S_V = \alpha \frac{p}{c'_P} \frac{|T_R|}{d_P} \frac{R}{\sqrt{1+(\omega CR)^2}} v_V \tag{17}$$

with $R = r_P \,//\, r_{eV}$ (18)

$C = C_P + C_{eV}$ (19)

The electrical time constant is given by:

$$\tau_E = CR \quad . \tag{20}$$

For many detectors $|T_R| \approx 1$, $(\omega CR)^2 >> 1$ and $C_P >> C_{eV}$ are valid. Then equation (17) simplifies considerably:

$$S_V = \alpha \frac{p}{c'_P \varepsilon_r} \frac{v_V}{\varepsilon_o \omega A_S} \tag{21}$$

In this case, responsivity is indirectly proportional to the modulation frequency.

The responsivity in current mode is given by:

$$S_V = \alpha \frac{p}{c'_P} \frac{|T_R|}{d_P} \frac{R_{GK}}{\sqrt{1+(\omega C_{GK} R_{GK})^2}} \tag{22}$$

If $|T_R| \approx 1$ and $(\omega C_{GK} R_{GK})^2 << 1$ are valid, the responsivity is independent of modulating frequency:

$$S_V = \alpha \frac{p}{c'_P} \frac{R_{GK}}{d_P} \tag{23}$$

If $(\omega C_{GK} R_{GK})^2 >> 1$, then

$$S_V = \alpha \frac{p}{c'_P} \frac{1}{d_P \omega C_{GK}} \quad . \tag{24}$$

6. Normalized noise voltage

Different noise sources exist in the pyroelectric detector. They produce a noise voltage at the output. The normalised noise voltage shares are:

$\widetilde{u}'_{RnT}$	noise voltage share, caused by the temperature noise source $\widetilde{p}_{RnT}$ of the responsive element
$\widetilde{u}'_{RnD}$	noise voltage share, caused by the tanδ noise source $\widetilde{i}_{RnD}$ of the responsive element
$\widetilde{u}'_{RnR}$	noise voltage share, caused by the thermal noise $\widetilde{i}_{RnR}$ of the input resistor r_{eV} of the preamplifier
$\widetilde{u}'_{RnI}$	noise voltage share, caused by the current noise $\widetilde{i}_{RnV}$ of the preamplifier
$\widetilde{u}'_{RnU}$	noise voltage share, caused by the voltage noise $\widetilde{u}_{RnV}$ of the preamplifier
$\widetilde{u}'_{RnGK}$	noise voltage share, caused by the thermal noise $\widetilde{i}_{RnGK}$ of the resistor R_{GK} of the preamplifier (only in the current mode of the preamplifier)

The whole normalized noise voltage at the preamplifier output arises from square addition of the noise voltage shares:

Preamplifier in voltage mode:

$$\widetilde{u}'^2_{Rn} = \widetilde{u}'^2_{RnT} + \widetilde{u}'^2_{RnD} + \widetilde{u}'^2_{RnR} + \widetilde{u}'^2_{RnI} + \widetilde{u}'^2_{RnU} \tag{25}$$

Preamplifier in current mode:

$$\widetilde{u}'^2_{Rn} = \widetilde{u}'^2_{RnT} + \widetilde{u}'^2_{RnD} + \widetilde{u}'^2_{RnR} + \widetilde{u}'^2_{RnI} + \widetilde{u}'^2_{RnU} + \widetilde{u}'^2_{RnGK} \tag{26}$$

The equations for the normalised noise voltage shares are arranged in table 1.

Table 1: Effective values of the normalised noise voltage shares at the preamplifier output

X	$\tilde{u}'_{RnX}$	
	voltage mode: $R = r_P \,//\, r_{eV}$, $C = C_P + C_{eV}$	current mode: $R` = r_P \,//\, r_{eV} \,//\, R_{GK}$, $C' = C_P + C_{eV} + C_{GK}$
T	$\frac{S_V}{\alpha}\sqrt{4kT^2G}$ (27)	
D	$\sqrt{4kT\omega C_P \tan\delta}\,\frac{R}{\sqrt{1+(\omega CR)^2}}\,v_V$ (28)	$\sqrt{4kT\omega C_P \tan\delta}\,\frac{R_{GK}}{\sqrt{1+(\omega C_{GK}R_{GK})^2}}$ (29)
R	$\sqrt{\frac{4kT}{r_{eV}}}\,\frac{R}{\sqrt{1+(\omega CR)^2}}\,v_V$ (30)	$\sqrt{\frac{4kT}{r_{eV}}}\,\frac{R_{GK}}{\sqrt{1+(\omega C_{GK}R_{GK})^2}}$ (31)
I	$\tilde{i}_{RnV}\,\frac{R}{\sqrt{1+(\omega CR)^2}}\,v_V$ (32)	$\tilde{i}_{RnV}\,\frac{R_{GK}}{\sqrt{1+(\omega C_{GK}R_{GK})^2}}$ (33)
U	$\tilde{u}_{RnV}\,v_V$ (34)	$\tilde{u}_{RnV}\,\frac{R_{GK}}{R'}\,\frac{\sqrt{1+(\omega C'R')^2}}{\sqrt{1+(\omega C_{GK}R_{GK})^2}}$ (35)
GK	-	$\sqrt{\frac{4kT}{R_{GK}}}\,\frac{R_{GK}}{\sqrt{1+(\omega C_{GK}R_{GK})^2}}$ (36)

7. Specific detectivity

The shares of the specific detectivity caused by the noise voltage shares result from the defining equation (3) of the specific detectivity as well as the basic equations of the responsivity (section 5) and normalized noise voltage (section 6):

D^*_T share of the specific detectivity, caused by the temperature noise source $\tilde{p}_{RnT}$ of the responsive element

D^*_D share of the specific detectivity, caused by the tan δ noise source $\tilde{i}_{RnD}$ of the responsive element

D^*_R share of the specific detectivity, caused by thermal noise $\tilde{i}_{RnR}$ of the input resistor r_{eV} of the preamplifier

D^*_I share of the specific detectivity, caused by the current noise $\tilde{i}_{RnV}$ of the preamplifier

D^*_U share of the specific detectivity, caused by the voltage noise

	$\widetilde{u}_{RnV}$ of the preamplifier
D^*_{GK}	share of the specific detectivity, caused by the thermal noise $\widetilde{i}_{RnGK}$ of the resistor R_{GK} of the preamplifier (only in the current mode of the preamplifier)

The whole specific detectivity is given by:

Preamplifier in voltage mode:

$$\left(\frac{1}{D^*}\right)^2 = \left(\frac{1}{D^*_T}\right)^2 + \left(\frac{1}{D^*_D}\right)^2 + \left(\frac{1}{D^*_R}\right)^2 + \left(\frac{1}{D^*_I}\right)^2 + \left(\frac{1}{D^*_U}\right)^2 \tag{37}$$

Preamplifier in current mode:

$$\left(\frac{1}{D^*}\right)^2 = \left(\frac{1}{D^*_T}\right)^2 + \left(\frac{1}{D^*_D}\right)^2 + \left(\frac{1}{D^*_R}\right)^2 + \left(\frac{1}{D^*_I}\right)^2 + \left(\frac{1}{D^*_U}\right)^2 + \left(\frac{1}{D^*_{GK}}\right)^2 \tag{38}$$

Table 2 contains the equations for the individual shares of the specific detectivity.

Table 2: Shares of the specific detectivity

X	D_X^*	Remarks
T	$\alpha\sqrt{\frac{A_S}{4kT^2G}}$ (39)	
D	$\alpha\frac{p}{c'_P\sqrt{\varepsilon_r\tan\delta}}\frac{1}{\sqrt{4kT\varepsilon_o\omega d_P}}\lvert T_R\rvert$ (40)	
R	$\alpha\frac{p}{c'_P}\sqrt{\frac{r_{eV}}{4kT}}\frac{\sqrt{A_S}}{d_P}\lvert T_R\rvert$ (41)	
I	$\alpha\frac{p}{c'_P}\frac{\sqrt{A_S}}{\tilde{i}_{RnV}d_P}\lvert T_R\rvert$ (42)	
U	$\alpha\frac{p}{c'_P}\frac{R}{\sqrt{1+(\omega CR)^2}}\frac{\sqrt{A_S}}{\tilde{u}_{RnV}d_P}\lvert T_R\rvert$ (43)	voltage mode: $R = r_P // r_{eV}$ $C = C_P + C_{eV}$
	$\alpha\frac{p}{c'_P}\frac{R'}{\sqrt{1+(\omega C'R')^2}}\frac{\sqrt{A_S}}{\tilde{u}_{RnV}d_P}\lvert T_R\rvert$ (44)	current mode: $R` = r_P // r_{eV} // R_{GK}$ $C' = C_P + C_{eV} + C_{GK}$
	$\alpha\frac{p}{c'_P\varepsilon_r}\frac{1}{\varepsilon_o\tilde{u}_{RnV}\omega\sqrt{A_S}}\lvert T_R\rvert$ (45)	voltage mode: $(\omega CR)^2 >> 1$, $C_P >> C_{eV}$ current mode: $(\omega C'R')^2 >> 1$, $C_P >> C_{eV} + C_{GK}$
GK	$\alpha\frac{p}{c'_P}\sqrt{\frac{R_{GK}}{4kT}}\frac{\sqrt{A_S}}{d_P}\lvert T_R\rvert$ (46)	only in current mode

8. Examples

For the following detector layouts, frequency dependence of responsivity, normalized noise voltage and specific detectivity are represented in the figures 6 to 11.

Detector layout	voltage mode	current mode
Responsive element:		
Pyroelectric material	$LiTaO_3$	$LiTaO_3$
Responsive area A_S	2 x 2 mm^2	2 x 2 mm^2
Thickness of the element d_P	5 µm	5 µm
Absorption coefficient α	0,7	0,7
Normalised current responsivity T_R	1	1
Preamplifier:		
Input resistance r_{eV}	$10^{11}\,\Omega$	$10^{11}\,\Omega$
Input capacity C_{eV}	2 pF	2 pF
Gain v_V	1	-
Resistor R_{GK}	-	$10^{10}\,\Omega$
Capacity C_{GK}	-	0,2 pF
Current noise $\tilde{i}_{RnV}$ (10 Hz)	$5 \cdot 10^{-16}$ A/$Hz^{1/2}$	$5 \cdot 10^{-16}$ A/$Hz^{1/2}$
Voltage noise $\tilde{u}_{RnV}$ (1 kHz)	6 nV/$Hz^{1/2}$	6 nV/$Hz^{1/2}$

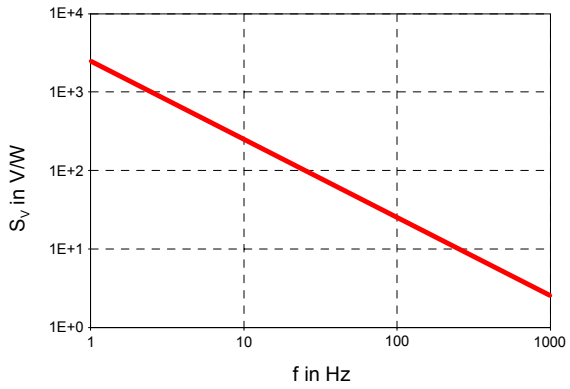

Figure 6: Frequency dependence of the responsivity at voltage mode

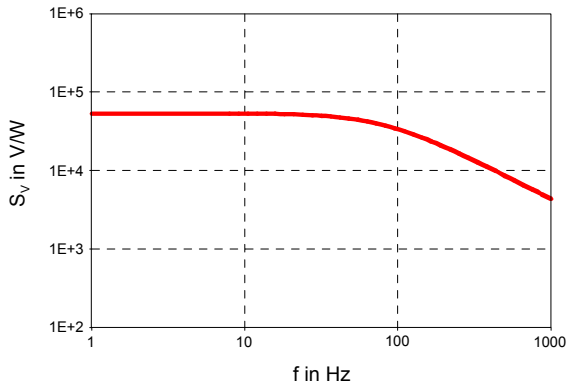

Figure 7: Frequency dependence of the responsivity at current mode

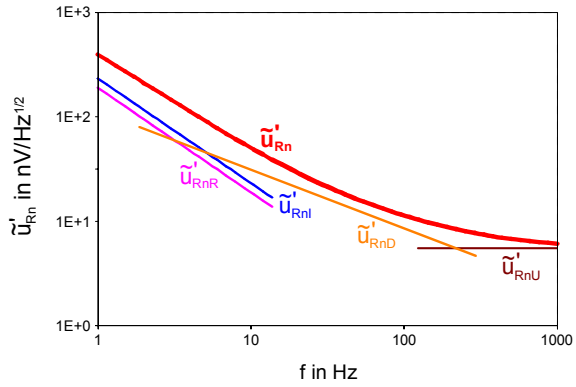

Figure 8: Frequency dependence of the normalized noise voltage at voltage mode

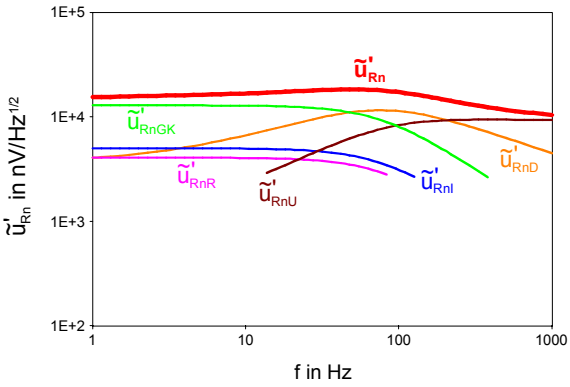

Figure 9: Frequency dependence of the normalized noise voltage at current mode

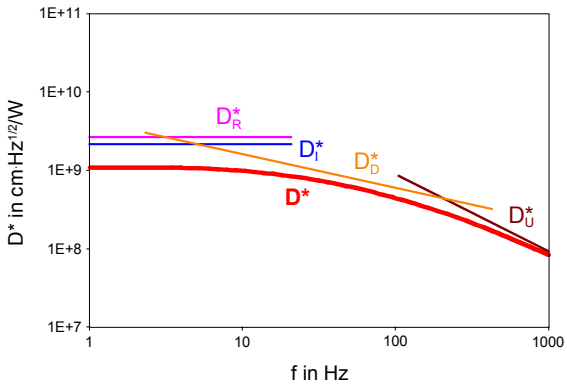

Figure 10: Frequency dependence of the specific detectivity at voltage mode

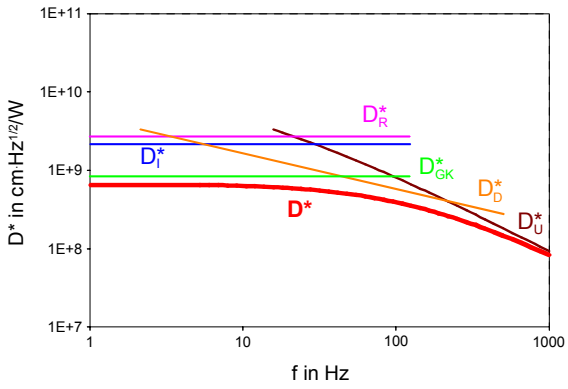

Figure 11: Frequency dependence of the specific detectivity at current mode